

Time-domain broadband phase-only full-waveform inversion with implicit shaping

Musa Maharramov*, Anatoly I. Baumstein, Yaxun Tang, Partha S. Routh, Sunwoong Lee, and Spyros K. Lazaratos, ExxonMobil Upstream Research Company

SUMMARY

We propose a new full-waveform inversion (FWI) method that approximates broadband tomographic inversion and has a reduced sensitivity to errors in the observed-data amplitude information. The method is based on fitting the observed-data phase spectrum while automatically shaping forward-modeled wave fields to the observed-data amplitude spectrum. This is achieved by using a phase-only objective function that allows broadband time-domain inversion of the observed-data phase information. We demonstrate our method's reduced sensitivity to dynamic information under the traveltimes approximation, and compare the new objective function to the normalized L_2 FWI objective function in an experiment on synthetic data with a frequency-dependent attenuation.

INTRODUCTION

Inversion of subsurface velocity models from seismic data using both phase and amplitude content of the observed data is sensitive to data quality and accuracy of the underlying mathematical model of wave propagation. For example, inverting amplitude-versus-offset (AVO) effects requires full elastic modeling; anisotropic phase-and-amplitude FWI requires accurate modeling of wavefield amplitudes in anisotropic media; unknown or changing amplitude spectra of the source often need to be taken into account to resolve subtle (for example, time-lapse) effects; transmission or absorption attenuation effects may easily leak into the inverted velocity models unless an adequate Q model is used. However, a good deal of information about subsurface velocity models can be, and routinely is, extracted from purely kinematic data, such as arrival times. Tomographic techniques based on this approach are very successful in practice and form the backbone of many existing velocity model building methods, but may require a significant amount of manual picking and analysis. Our objective is to achieve automated time-domain full-waveform inversion of subsurface velocity models using mostly kinematic information contained in broadband seismic data, while largely ignoring dynamic (amplitude) information.

One approach to constructing true kinematic FWI objective functions is based on extracting traveltimes differences between the observed and predicted data by cross-correlation (Luo and Schuster, 1991; Gee and Jordan, 1992; Van Leeuwen and Mulder, 2010), and is sensitive to noise in the data and ambiguity in event picking. Another approach is based on constructing phase and amplitude misfits in time and frequency domains (Fichtner and Igel, 2008; Bozdağ et al., 2011; Fichtner, 2011). The latter approach, as well as the normalized L_2 FWI (Routh et al., 2011), do not fully separate kinematic and dynamic information, but provide an approximation to kinematic inversion by using phase as a proxy for traveltimes information.

However, due to the lack of full separation, amplitude errors in the observed or predicted data leak into the inversion result, limiting the utility of such methods. In this work we propose an objective function for a broadband FWI that fully separates kinematic and dynamic information for a single transmission or reflection event even in cases of dispersive propagation. We demonstrate that the proposed method still outperforms a popular alternative in a realistic example with multiple reflection and transmission events, and in the presence of amplitude attenuation.

THEORY

Our method is based on minimizing the following objective function that represents a weighted phase misfit between the observed and forward-modeled data:

$$\left\| \hat{d} \left(\frac{\hat{u}}{|\hat{u}|} - \frac{\hat{d}}{|\hat{d}|} \right) \right\|^2 = \int \left| \hat{d} \left(\frac{\hat{u}}{|\hat{u}|} - \frac{\hat{d}}{|\hat{d}|} \right) \right|^2 d\omega, \quad (1)$$

where $d = d(t, s, r)$ stands for the observed data trace for a single source-receiver pair s, r , and $u = u(t, s, r)$ is predicted (forward-modeled) data. The "hats" above the wave field symbols denote temporal Fourier transforms. Note that in the above objective function the amplitude spectrum of the predicted data is shaped to the amplitude spectrum of the observed data, thus always matching it. Ignoring multipathing (i.e., assuming a single transmitted or reflected wave) the observed data response to a delta-function source is asymptotically given by the following traveltimes (high-frequency or WKB) approximation:

$$\hat{d}(\omega, s, r) = A_d(\omega, s, r) \exp[i\omega\tau_d(\omega, s, r)], \quad (2)$$

where $\tau_d(\omega, s, r)$ is the observed traveltimes between source s and receiver r , and $A_d(\omega, s, r)$ is the observed wave field amplitude. Note that in Equation 2 we allow frequency-dependent kinematic and dynamic propagation effects, such as attenuation due to transmission and absorption. Similarly, for the forward-modeled wave field, we have

$$\hat{u}(\omega, s, r) = A_u(\omega, s, r) \exp[i\omega\tau_u(\omega, s, r)]. \quad (3)$$

Substituting Equations 2 and 3 into Equation 1, for the misfit functional we obtain

$$\int A_d^2 |\exp[i\omega\tau_u] - \exp[i\omega\tau_d]|^2 d\omega, \quad (4)$$

where the dependence of A_d , τ_d , and τ_u on ω , s , and r is omitted for brevity. The integrand in Equation 4 is a measure of the misfit between the observed and predicted traveltimes τ_d and τ_u modulo $2\pi/\omega$, weighted by the observed wave field amplitude. The objective function becomes zero if the traveltimes is accurately predicted regardless of any errors in either forward-modeled A_u or observed A_d amplitudes. In this sense

Time-domain broadband phase-only FWI with implicit shaping

Equation 1 provides a true “kinematic” objective function under the assumption of single-event asymptotic representations in Equations 2 and 3. Of course, instead of Equation 1 we can use a simple frequency-domain normalized misfit

$$\left| \frac{\hat{u}}{|\hat{u}|} - \frac{\hat{d}}{|\hat{d}|} \right|^2 \quad (5)$$

in either time or frequency-domain FWI. As with Equation 1, Equation 5 provides an amplitude-insensitive objective function for fitting single events of Equations 2 and 3. However, our proposed objective function in Equation 1 provides a broadband inversion over an arbitrary range of frequencies with the data amplitude spectrum acting as a frequency-dependent misfit weight. Any desired shaping can be applied to the observed data amplitude spectrum in a single data preprocessing step, for example, boosting lower frequencies to improve FWI convergence and reduce sensitivity to cycle skips (Lazaratos et al., 2011; Plessix and Li, 2013). Another advantage of the new objective function is its ability to handle singularities in the normalized observed wave field due to notches in the amplitude spectrum in the presence of complex multipathing. In any realistic experiment the observed wave field is the sum of multiple events of Equation 2, representing various transmitted and reflected waves,

$$\hat{d}(\omega, s, r) = \sum_j A_d^j(\omega, s, r) \exp \left[i\omega \tau_d^j(\omega, s, r) \right], \quad (6)$$

with various traveltimes τ_d^j and amplitudes A_d^j . Complex multipathing may result in the amplitude spectrum of the multiple-event trace of Equation 6 being close to zero, leading to errors in the normalized wave fields in Equations 1 and 5. Weighting of the integrand in Equation 1 by the observed data amplitude spectrum effectively eliminates the contribution of such singularities. It must be noted that when a single-event asymptotic of Equation 2 is not valid, our method can no longer be regarded as a true kinematic inversion. Indeed, the phase spectrum of a multiple-event trace in Equation 6 is determined by both traveltimes and amplitudes of the individual events. Amplitude errors in either forward-modeled or observed data leak into the phase spectrum and inverted models, reducing contribution of the weakest events to the inversion. This obvious limitation of the proposed method can be partially overcome using data masking for isolating individual events of interest as, for example, in a target-oriented or time-lapse inversion. One existing broadband alternative to the proposed method is the normalized L_2 objective function (Routh et al., 2011),

$$\left\| \frac{u}{\|u\|} - \frac{d}{\|d\|} \right\|^2 = \int \left\| \frac{u}{\|u\|} - \frac{d}{\|d\|} \right\|^2 dt. \quad (7)$$

For a single-event asymptotic of Equation 2 and in the absence of frequency dispersion—i.e., when both traveltime τ_d and amplitude A_d are independent of ω —the normalized L_2 objective function of Equation 7 yields a purely kinematic misfit equivalent to that of Equation 1. However, for a dispersive propagation with the amplitude A_d as a function of frequency, or in the presence of a frequency-dependent noise, division by the full trace norm in Equation 7 may not completely remove dynamic

effects, resulting in a leakage of amplitude information into the misfit. If forward modeling is not dynamically accurate, this leakage may result in significant inversion errors.

EXAMPLES

We conduct time-domain full-waveform inversion experiments with the objective functions in Equations 1 and 7 using synthetic data with and without amplitude attenuation. The adjoint source for the new objective function is computed as

$$f(t, s, r) = \mathcal{F}_{\omega \rightarrow t}^{-1} \left\{ \frac{2i}{\hat{u}} \text{Im} [w\bar{\hat{u}}(w\hat{u} - \hat{d})] \right\} \quad (8)$$

where $w(\omega) = |\hat{d}|/|\hat{u}|$ and $\mathcal{F}_{\omega \rightarrow t}^{-1}$ is the inverse Fourier transform. We generated synthetic data using acoustic modeling with density. The true velocity model used in our experiments is shown in Figure 1, the true density model is obtained from the true velocity model by dividing it by 1500 (setting water density to 1). Both forward modeling and inversion are performed on a 1000 (horizontal) by 800 (vertical) computational grid with a 10 m horizontal and 5 m vertical spacing. A Ricker wavelet centered at 10 Hz is used for source, and absorbing boundary conditions are applied at the surface to avoid surface-related multiples. A streamer acquisition is used with 39 shots and a 260 m shot spacing, with offsets ranging from 10 m to 10 km. We use a starting velocity model obtained from the true model using a 400 m smoothing filter.

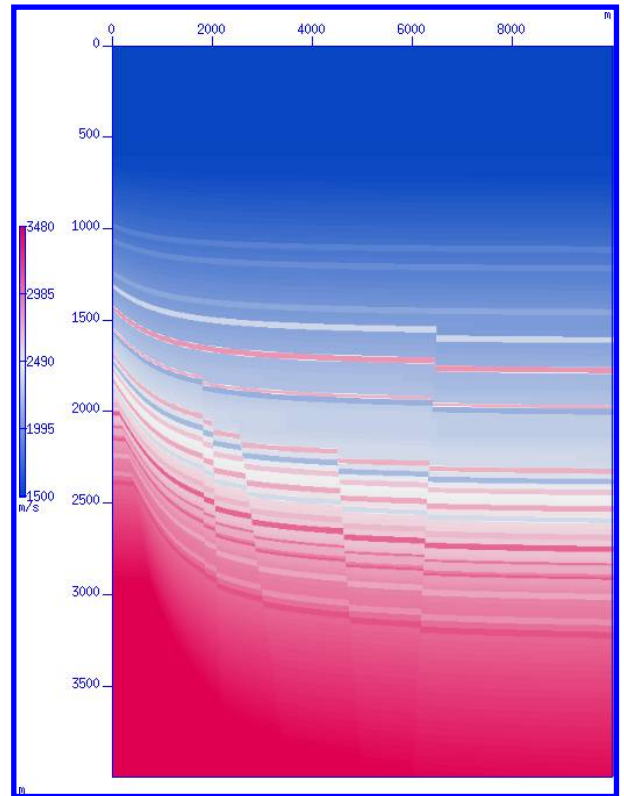


Figure 1: The true velocity model. The true density model was obtained from velocity by dividing it by 1500.

Time-domain broadband phase-only FWI with implicit shaping

We use no frequency continuation and conduct a 0-25 Hz broadband time-domain full-waveform inversion to convergence, using the objective functions of Equations 1 and 7. In our experiments we intentionally avoid density inversion in order to study the effect of amplitude errors on our objective functions. Since the true model generates multiple refraction and reflection events, the neglected density effects are expected to leak into the velocity inversion. Indeed, for the acoustic reflection coefficient in the absence of elastic conversions, for small reflection angles less than $\approx 30^\circ$ we have (Aki and Richards, 1980; Shuey, 1985):

$$R(\theta) \approx \frac{1}{2} \left(\frac{\Delta V_P}{V_P} + \frac{\Delta \rho}{\rho} \right) + \sin^2 \theta \frac{1}{2} \frac{\Delta V_P}{V_P}, \quad (9)$$

where θ is the reflection angle, V_P and ρ are the acoustic velocity and density below a model contrast, and ΔV_P and $\Delta \rho$ are velocity and model changes across the model contrast.

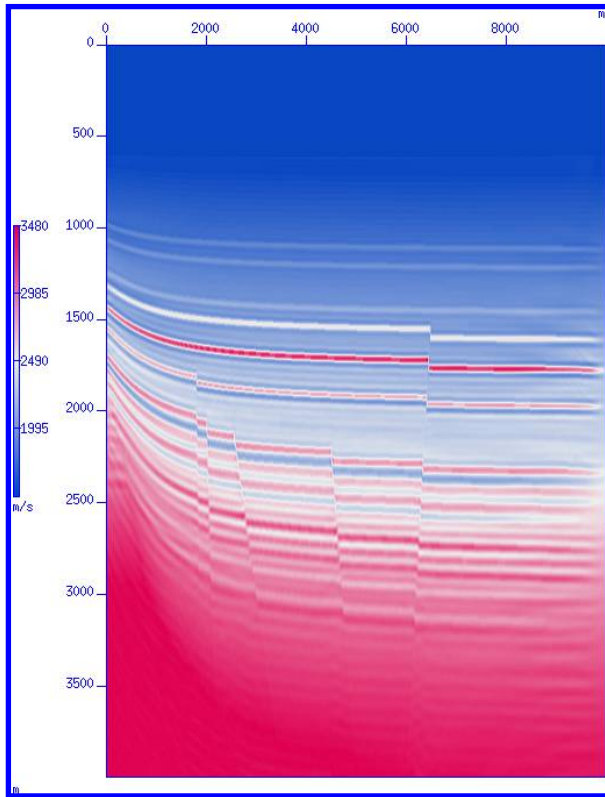


Figure 2: The inverted velocity model using the objective function of Equation 1. Density was not inverted and non-constant density effects leaked into the inverted velocity, resulting in sharper model contrasts.

Equation 9 demonstrates that with our choice of the true density model, density contrasts boost the amplitude effects of velocity contrasts, especially at near offsets, and the leakage of density into the inverted acoustic velocity model should result in sharper velocity contrasts. Figure 2 shows the acoustic velocity model obtained by FWI with the proposed phase-only objective function of Equation 1. As expected, the inversion exhibits a good qualitative agreement with the true ve-

locity model of Figure 1, however, velocity contrasts are over-predicted. FWI using the normalized L_2 objective function of Equation 7 produced a similar result with no clear advantage to any method, as demonstrated by the forward-modeled traces shown in Figure 3. In the absence of frequency dispersion, both approaches deliver similar results, and both suffer from amplitude leakage into the phase spectrum of multiple-event traces in Equation 6.

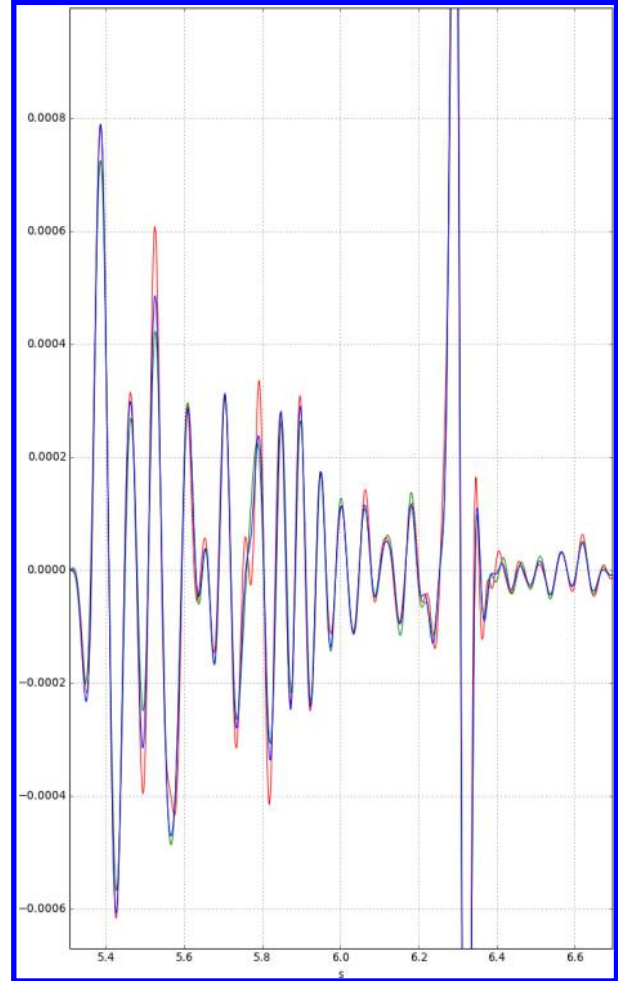


Figure 3: Predicted traces at ≈ 1 km offset using Equation 1 (green) and Equation 7 (blue) versus unattenuated true data (red). In the absence of frequency dispersion the normalized L_2 produces results comparable to those obtained using the new objective function.

In our next experiment we apply amplitude attenuation to the synthetic data of the previous experiment using a uniform Q constant of 60. No phase effects of Q are applied as our objective is to mimic kinematically accurate propagators with dynamic errors in either data or the propagator. FWI using Equation 1 produced both qualitatively and quantitatively superior results across all depths as shown in a sample velocity log of Figure 4.

While both methods suffer from amplitude leakage, the phase-

Time-domain broadband phase-only FWI with implicit shaping

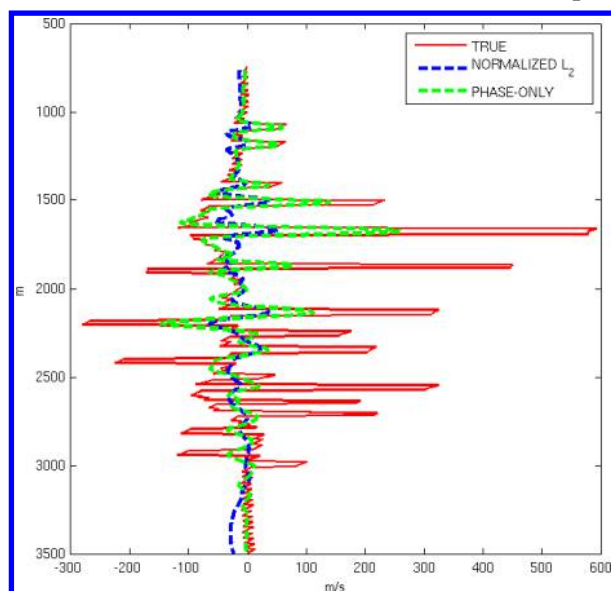


Figure 4: Logs of the velocity difference from the starting velocity at 1 km inline coordinate using FWI with Equation 1 (green), Equation 7 (blue), and true velocity model (red). The phase-only objective function with implicit shaping delivers a more accurate velocity across all depths in comparison with the normalized L_2 FWI.

only objective function with implicit shaping can at least correctly separate phase and amplitude information for single events, resulting in a reduced sensitivity to amplitude errors, especially for weaker events. This is demonstrated in Figure 5, which shows forward-modeled data traces versus unattenuated true data. The normalized L_2 FWI appears to be most sensitive to the strongest events, while the new phase-only method delivers a better overall kinematic agreement.

CONCLUSIONS

FWI based on our new phase-only objective function with implicit shaping can achieve time-domain broadband inversion of subsurface models from the phase spectrum of the observed data. While in the presence of multipathing the method does not deliver a true kinematic inversion, it is less sensitive to frequency dispersion in the amplitude information in comparison with the normalized L_2 . The new method can deliver qualitatively and quantitatively better results in the presence of attenuation and other dispersive phenomena. Implicit shaping to the observed-data amplitude spectrum provides frequency-dependent weighting of phase misfits and can help avoid computationally expensive frequency continuation in time-domain FWI. Applications of the proposed method can include FWI using kinematically accurate but dynamically wrong numerical propagators (for example, pseudo-acoustic anisotropic propagators), inversion of field data with noisy or unreliable amplitude information, kinematic source inversion, and time-lapse FWI. Application of the proposed method to time-lapse FWI may be of particular interest, providing a broadband alterna-

tive to the frequency-continuation approach based on the misfit functional of Equation 5 as described by Maharramov et al. (2016).

ACKNOWLEDGMENTS

The authors would like to thank Ramesh Neelamani, Ganglin Chen, Tom Dickens, David Johnston, and Eric Wildermuth for a number of useful discussions, and ExxonMobil Upstream Research Company for the permission to publish this work.

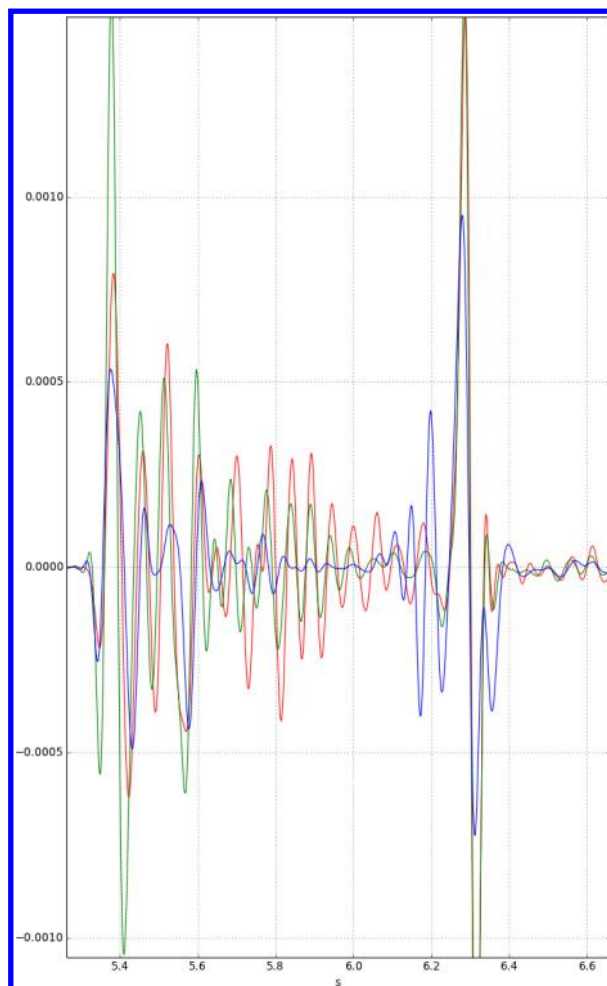


Figure 5: Predicted traces at ≈ 1 km offset using FWI velocity models from attenuated data with $Q = 60$ and the objective functions of Equation 1 (green) and Equation 7 (blue) versus the unattenuated true data (red). In the presence of frequency dispersion the new method achieves a better kinematic accuracy in comparison with the normalized L_2 FWI.

EDITED REFERENCES

Note: This reference list is a copyedited version of the reference list submitted by the author. Reference lists for the 2017 SEG Technical Program Expanded Abstracts have been copyedited so that references provided with the online metadata for each paper will achieve a high degree of linking to cited sources that appear on the Web.

REFERENCES

- Aki, K., and P. G. Richards, 1980, Quantitative seismology: Theory and methods: W. H. Freeman and Co.
- Bozdag, E., J. Trampert, and J. Tromp, 2011, Misfit functions for full waveform inversion based on instantaneous phase and envelope measurements: *Geophysical Journal International*, **185**, 845–870, <http://dx.doi.org/10.1111/j.1365-246X.2011.04970.x>.
- Fichtner, A., 2011, Full seismic modeling and inversion: Springer.
- Fichtner, A., and H. Igel, 2008, Efficient numerical surface wave propagation through the optimization of discrete crustal models — a technique based on non-linear dispersion curve matching (DCM): *Geophysical Journal International*, **173**, 519–533, <http://dx.doi.org/10.1111/j.1365-246X.2008.03746.x>.
- Gee, L. S., and T. H. Jordan, 1992, Generalized seismological data functionals: *Geophysical Journal International*, **111**, 363–390, <http://dx.doi.org/10.1111/j.1365-246X.1992.tb00584.x>.
- Lazaratos, S., I. Chikichev, and K. Wang, 2011, Improving the convergence rate of full wavefield inversion using spectral shaping: 81st Annual International Meeting, SEG, Expanded Abstracts, 2428–2432, <http://dx.doi.org/10.1190/1.3627696>.
- Luo, Y., and G. T. Schuster, 1991, Wave-equation traveltime inversion: *Geophysics*, **56**, 645–653, <http://dx.doi.org/10.1190/1.1443081>.
- Maharramov, M., B. L. Biondi, and M. A. Meadows, 2016, Time-lapse inverse theory with applications: *Geophysics*, **81**, no. 6, R485–R501, <http://dx.doi.org/10.1190/geo2016-0131.1>.
- Plessix, R.-E., and Y. Li, 2013, Waveform acoustic impedance inversion with spectral shaping: *Geophysical Journal International*, **195**, 301–314, <http://dx.doi.org/10.1093/gji/ggt233>.
- Routh, P. S., J. R. Krebs, S. Lazaratos, A. I. Baumstein, I. Chikichev, N. Downey, D. Hinkley, and J. E. Anderson, 2011, Full-wavefield inversion of marine streamer data with the encoded simultaneous source method: 73rd Annual International Conference and Exhibition, EAGE, Extended Abstracts, F032, <http://dx.doi.org/10.3997/2214-4609.20149730>.
- Shuey, R. T., 1985, A simplification of the Zoeppritz equations: *Geophysics*, **50**, 609–614, <http://dx.doi.org/10.1190/1.1441936>.
- Van Leeuwen, T., and W. A. Mulder, 2010, A correlation-based misfit criterion for wave-equation traveltime tomography: *Geophysical Journal International*, **182**, 1383–1394, <http://dx.doi.org/10.1111/j.1365-246X.2010.04681.x>.